Supporting Information

Enzyme-Controlled Nitrogen-Atom Transfer Enables Regiodivergent C–H Amination

Todd K. Hyster, Christopher C. Farwell, Andrew R. Buller, John A. McIntosh, Frances H. Arnold

Experimental Procedures

General. Unless otherwise noted, all chemicals and reagents for chemical reactions were obtained from commercial suppliers (Sigma-Aldrich, VWR, Alfa Aesar) and used without further purification. Silica gel chromatography purifications were carried out using AMD Silica Gel 60, 230-400 mesh. ^{1}H and ^{13}C spectra were recorded on a Varian Inova 500 MHz instrument in DMSO, and are referenced to the residual solvent peak. Synthetic reactions were monitored using thin layer chromatography (Merck 60 gel plates) using an UV-lamp for visualization.

Chromatography. Analytical high-performance liquid chromatrography (HPLC) was carried out using an Agilent 1200 series. Total turnover numbers were determined on a Kromasil 100 C18 column (Peeke Scientific 4.6 x 50 mm, 5 μm) column measured against an 1,3,5-trimethoxybenzene as an internal standard with H_2O and acetonitrile as the mobile phase. Regioselectivity was determined on an Agilent XDB-C18 column (9.4 x 250 mm, 5 μm) at 230 nm with H_2O and methanol as the mobile phase. Analytical chiral HPLC was conducted using a supercritical fluid chromatography (SFC) system with isopropanol and liquid CO_2 as the mobile phase. Chiral OD-H and AD-H columns were used to separate the sultam enantiomers (4.6 x 150 mm, 5 μm). Sultam standards were prepared as reported.[1]

Cloning and site-directed mutagenesis. pET22b(+) was used as a cloning and expression vector for all enzymes described in this study. Site-directed

mutagenesis was performed using a modified QuikChange™ mutagenesis protocol. The PCR products were gel purified, digested with DpnI, repaired using Gibson Mix™, and directed transformed into *E. coli* strain BL21(DE3).

Determination of P450 concentration. Concentration of P450/P411 enzymes was determined from ferrous carbon monoxide binding difference spectra using previously reported extinction coefficients for cysteine-ligated (ε = 91,000 $M^{-1}cm^{-1}$) and serine-ligated enzymes (ε = 103,000 M^{-1} cm^{-1}).

Protein expression and purification. Enzymes used in purified protein experiments were expressed in BL21(DE3) *E. coli* cultures transformed with plasmid encoding P450 or P411 variants. Expression and purification was performed as described except that the shake rate was lowered to 130 RPM during expression.[2] Following expression, cells were pelleted and frozen at -20 °C. For purification, frozen cells were resuspended in buffer A (20 mM tris, 20 mM imidazole, 100 mM NaCl, pH 7.5, 4 mL/g of cell wet weight) and disrupted by sonication (2 x 1 min, output control 5, 50% duty cycle; Sonicator 3000, Misonix, Inc.). To pellet insoluble material, lysates were centrifuged at 24,000 x g for 0.5 h at 4 °C. Proteins were expressed in a construct containing a 6x-His tag and were consequently purified using a nickel NTA column (5 mL HisTrap HP, GE Healthcare, Piscataway, NJ) using an AKTAxpress purifier FPLC system (GE healthcare). P450 or P411 enzymes were then eluted on a linear gradient from 100% buffer A 0% buffer B (20 mM tris, 300 mM imidazole, 100 mM NaCl, pH 7.5) to 100 % buffer B over 10 column volumes (P450/P411 enzymes elute at

around 80 mM imidazole). Fractions containing P450 or P411 enzymes were pooled, concentrated, and subjected to three exchanges of phosphate buffer (0.1 M KPi pH 8.0) to remove excess salt and imidazole. Concentrated proteins were aliquoted, flash-frozen on powdered dry ice, and stored at -20 °C until later use.

Reaction screening in 96-well plate format. Site-saturation libraries were generated by employing the "22c-trick" method.[3] *E. coli* libraries were generated and culture in 200 µL of LB_{AMP} and stored as glycerol stocks at -80 ºC in 96-well plates. 50 µL of the preculture was transferred to a 1200 µL of Hyperbroth using a multichannel pipette. The cultures were incubated at 37 ºC, 200 rpm, 80% humidity until the OD_{600} = 4 (approx. 2.5 hours). The plates were cooled on ice for 30 minutes before expression was induced (0.5 mM IPTG, 1mM Ala final concentration. Expression was conducted at 20 ºC, 180 rpm, 20 h. The cells were pelleted (4000g, 10 min, 4 ºC) and the 96-well plate was transferred to an anaerobic chamber. The pellets were resuspended in 300 µL argon sparged reaction buffer (4:1 M9-N/glucose (250 mM)). GOX solution (10x, 40 µL/well) was added to each well followed by azide **1** (100 mM, 10 µL/well). The plate was sealed with aluminum sealing tape, removed from the anaerobic chamber, and shaken at 40 rpm. After 12 hours, the seal was removed and 500 µL of acetonitrile and 10 µL of standard (10 mM) were added to each well. The plate was vortexed and centrifuged (4000g, 30 minutes) and 500 µL aliquots were transferred to a shallow-well plate for analysis by HPLC.

Typical procedure for small-scale amination bioconversions under anaerobic conditions using whole cells. *E. coli* BL21(DE3) cells containing P450 or P411 enzymes were expressed and resuspended to an OD_{600}=30 in M9-N), and then degassed by sparging with argon in a sealed 6 mL crimp vial for at least 30 mintues. Separately, glucose (250 mM dissolved in 1X M9-N, 40 µL, or multiples thereof) was degassed by sparging with argon for at least five minutes. The oxygen quenching mixture (40 µL) was added to a 2 mL crimp vial containing stir bars. All solutions were uncapped and transferred into an anaerobic chamber. Resuspended cells (300 µL) were added to the vial containing the oxygen quenching mixture, followed by glucose (50 µL), and substrate (100 mM arylsulfonyl azide, 10 µL in DMSO). The vial was sealed, removed from the anaerobic chamber and stirred at room temperature for 8h. The reactions were quenched by adding acetonitrile (450 µL) and internal standard (1,3,5 trimethoxybenzene (10 mM in DMSO). The mixture was then transferred to a microcentrifuge tube and centrifuged at 14,000 rpm for 10 minutes. The solution was transferred to an HPLC vial and analyzed by HPLC for yield and regioselectivity. For chiral HPLC the reactions were extracted with ethyl acetate, dried and resuspended in DMSO (100 µL) and then C18 purified to isolate the major regioisomer. The purified material was dried, resuspended in acetonitrile, and injected onto the chiral HPLC system for analysis.

Determination of initial rates. All initial rate experiments were set up in an anaerobic chamber. Four 2-ml vials were charged with a stir bar, GOX 10x (40 µL), glucose (250 mM, 40 µL), NADPH (20 mM, 40 µL), and KPi (pH = 8.0, 0.1

M, 260 µL). The vials were sealed with a silicon crimp cap and removed from the anaerobic chamber. The reactions were placed on a stir plate and charged with azide **1** or azide **1'** (100 mM, 10 µL). The reactions were quenched at 2-3 minute intervals over 8-12 minutes by decapping and adding acetone (500 µL) and internal standard (1,3,5-trimethoxybenzene 10 mM, 10 µL) . After 5 minutes of stirring, the reaction mixtures were transferred to 1.8 mL tubes, which were vortexed and centrifuged (14,000 x g, 10 min). The supernatant was transferred to a vial for analysis by HPLC. TTNs were plotted as a function of time for the proteo- and deutero-substrate and compared to determine the ^{1}H-KIE for P411$_{BM3}$-CIS-T438S-I263F and P411$_{BM3}$-T268A-F87A (Figures S2 and S3).

Crystallization, data collection, and structure determination. The heme domain of P411BM3-CIS-T438S-I263F was purified, flash frozen in liquid N_2, and stored at -80 °C until crystallization. Sitting drop vapor diffusion experiments were performed by generating a 1:1 mixture of protein stock (12 mg/mL in 0.1 M KPi, pH = 8.0) and well solution in a 96-well sitting-drop plate with a final drop volume of 0.4 µL and a reservoir volume of 400 µL. Crystals grew over 5-10 days in 0.1 M Tris/HCl (pH = 7.0), 2.0 M ammonium sulfate, 0.2 M lithium sulfate. Crystals were cryoprotected by immersion into well solution with 20% glycerol before being flash-frozen in liquid N_2. Diffraction data were collected on the Stanford Synchrotron Radiation Laboratory Beamline 12-2. Data were processed using XDS in the spacegroup $P4_22_12$ to 2.66 Å resolution.[4]

The structure of P411BM3-CIS-T438S-I263F was solved by molecular replacement using the Phaser program,[5] as implemented in CCP4,[6] using the

P411BM3-CIS structure [PDB ID: 4H23] as the search model. Model building was performed in Coot and restrained refinement in Refmac5.[7] Model quality was assessed with the MolProbity online server.[8] TLS operators were included in the last round of refinement.[9] Crystallographic and model statistics are described in Table S1.

Table S1. Data processing and refinement statistics (PDB=4WG2)

Data processing	P411BM3-CIS-T438S-I263F
Wavelength	
Spacegroup	$P4_22_12$
Unit cell dimensions	= 90°
a = b , c	206.9 , 119.39
α = β = γ	90
Beamline	SSRL 12-2
Wavelength	0.9795 Å
Resolution (Å)	39.1 – 2.66
Last bin (Å)	2.8 – 2.66
Number of Observations	1,031,477
Completeness (%)	100 (100)
R_{meas} (%)	0.25 (2.1)
R_{pim} (%)	0.067 (0.550)
I/σI	11.0 (1.44)
CC1/2	0.996 (0.534)
Redundancy	13.8 (14.5)
Refinement	
Number of reflections	70732
Number of atoms	10947
Last bin (Å)	2.73 – 2.66
R_{work}	19.7 (34.7)
R_{free}	23.5 (37.5)
Average B factor (Å^2)	36.2
Ramachandran Plot	
Most favored (%)	96.4
Allowed (%)	99.9
Outliers (%)	0.1

Values in parenthesis are for the highest resolution shell
R_{merge} is Σ|Io – I| / ΣIo , where Io is the intensity of an individual reflection, and I is the mean intensity for multiply recorded reflections
Rpim is 1/(N-1) Σ|Io – I| / ΣIo, where N is the number of observations for a given reflection
R_{work} is ||Fo – Fc|| / Fo, where Fo is an observed amplitude and Fc a calculated amplitude;
R_{free} is the same statistic calculated over a 5.1% subset of the data that has not been included during refinement.

Sultams **2** and **3** were previously reported by Katsuki.[10]

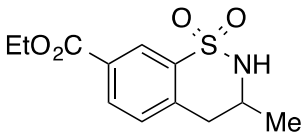

ethyl 3-methyl-3,4-dihydro-2*H*-benzo[*e*][1,2]thiazine-7-carboxylate 1,1-dioxide (9)

^{1}H 500 MHz (DMSO d_6): 8.17 (d, 1H, J=1.8 Hz), 8.06 (d, 1H, J=1.8, 8.2 Hz), 7.53 (m, 2H), 4.34 (q, 2H, J=7.25 Hz), 3.83 (m, 1H), 3.06 (dd, 1H, J=17.6, 3.7 Hz), 2.79 (dd, 1H, J=17.6, 11.4 Hz), 1.34 (3H, t, J=7.1 Hz), 1.28 (3H, d, J=6.6 Hz).

^{13}C 125 MHz (DMSO d_6): 164.4, 141.4, 137.9, 131.8, 130.7, 128.9, 123.7, 61.3, 48.6, 34.9, 21.0, 14.1.

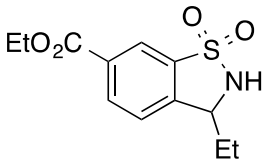

ethyl 3-ethyl-2,3-dihydrobenzo[*d*]isothiazole-6-carboxylate 1,1-dioxide (10)

^{1}H 500 MHz (DMSO d_6): 8.23 (dd, 1H, J=8.1, 1.5 Hz), 8.20 (d, 1H, J=1.5 Hz), 8.16 (d, 1H, J=4.2 Hz), 7.77 (d, 1H, J=8.1 Hz), 4.72 (ap p, 1H, J=4.0 Hz), 4.37 (q, 2H, J=7.1 Hz), 1.97 (m, 1H), 1.68 (m, 1H), 1.35 (t, 3H, J=7.1 Hz), 0.90 (t, 3H, J=7.3 Hz).

^{13}C 125 MHz (DMSO d_6): 164.3, 145.3, 136.9, 133.3, 131.1, 125.7, 121.1, 61.5, 58.2, 27.9, 14.1, 9.8.

TABLE S2: Mutations (relative to wild-type $P450_{BM3}$) in enzymes used in this study.

Enzyme	Mutations relative to wild-type $P450_{BM3}$
$P450_{BM3}$	None
$P411_{BM3}$-T268A	C400S-T268A
$P450_{BM3}$-CIS	V78A, F87V, P142S, T175I, A184V, S226R, H236Q, E252G, T268A, A290V, L353V, I366V, E442K
$P411_{BM3}$-CIS	$P450_{BM3}$-CIS C400S
$P411_{BM3}$-H2-5-F10	$P411_{BM3}$-CIS L75A, I263A, L437A
$P411_{BM3}$-H2-4-D4	$P411_{BM3}$-CIS M177A, L181A, L437A
$P411_{BM3}$-H2-A10	$P411_{BM3}$-CIS L75A, L181A
$P411_{BM3}$-CIS-T438S	$P411_{BM3}$-CIS T438S
$P411_{BM3}$-CIS-T438S-I263F	$P411_{BM3}$-CIS T438S, I263F
$P411_{BM3}$-CIS-T438S-I263F-A268T	$P411_{BM3}$-CIS T438S, I263F, A268T
$P450_{BM3}$-CIS-T438S-I263F	$P450_{BM3}$-CIS T438S, I263F
$P411_{BM3}$-MAN1-T268A	V78A, F81L, A82T, F87A, P142S, T175I, A184V, F205C, S226R, H236Q, E252G, R255S, A290V, L353V, C400S
$P411_{BM3}$-MAN1-T268A-M263I	V78L, F87A, P142S, T175I, A184T, F205C, S226R, H236Q, E252G, R255S, A290V, G315S, A330V, L353V, T268A, C400S
$P411_{BM3}$-T268A-F87A	C400S-T268A-F87A
$P411_{BM3}$-T268A-F87V	C400S-T268A-F87V
$P411_{BM3}$-CIS-T438S-I263F-F87A	$P411_{BM3}$-CIS T438S, I263F

TABLE S3: Mass Balance of Reactions

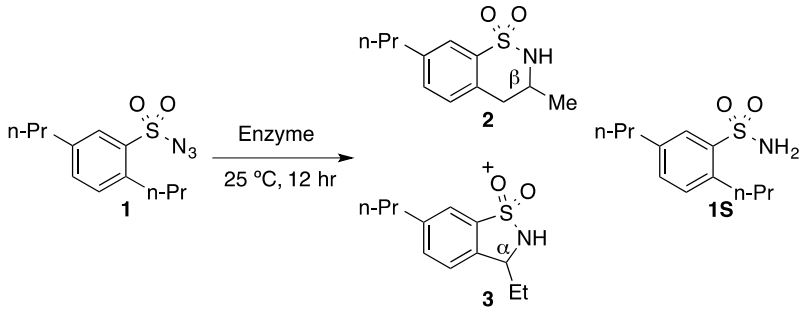

entry	Catalyst	Yield **2+3**	Yield **1S**
1	$P411_{BM3}$-CIS-T438S-I263F	54%	45%
2	$P411_{BM3}$-T268A-F87A	26%	44%

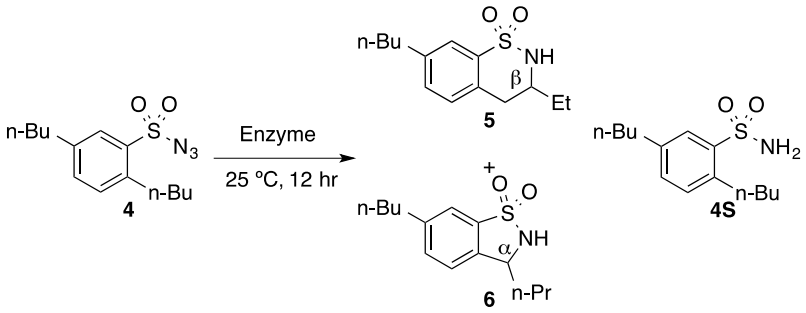

entry	Catalyst	Yield **5+6**	Yield **4S**
1	$P411_{BM3}$-CIS-T438S-I263F	18%	37%
2	$P411_{BM3}$-T268A-F87A	16%	46%

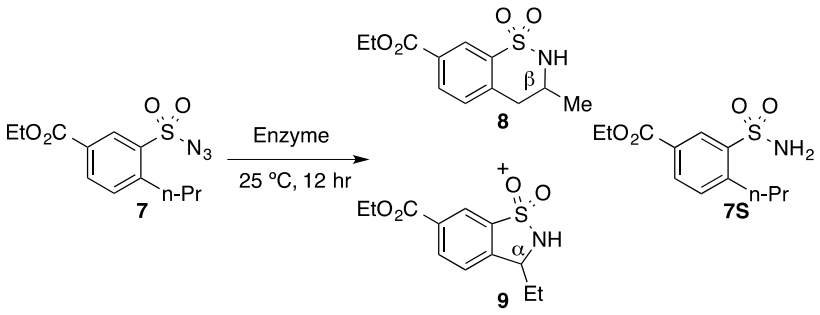

entry	Catalyst	Yield **5+6**	Yield **7S**
1	$P411_{BM3}$-CIS-T438S-I263F	15%	85%
2	$P411_{BM3}$-T268A-F87A	18%	82%

TABLE S4: Control Experiments.

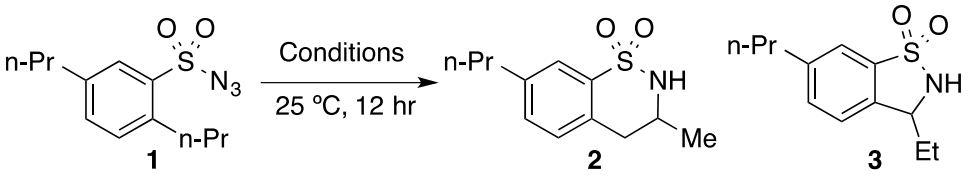

Conditions	TTN (2 + 3)
CS ($P411_{BM3}$-CIS-T438S-I263F)	361
Empty Vector	0
CS + CO	0
Hemin + $Na_2S_2O_4$	0
Hemin + $Na_2S_2O_4$ + BSA	0

Conditions for whole-cell catalysis – Cells resuspended to OD_{600} = 30 in M9-N (300 µL), GOX mixture (10x 14,000U catalase/1,000U glucose oxidase per mL) (40 µL), 250 mM Glucose (50 uL), 100 mM azide **1** (10 µL).

Table S5: Results with reactions run with purified protein and in lyophilized whole cells.

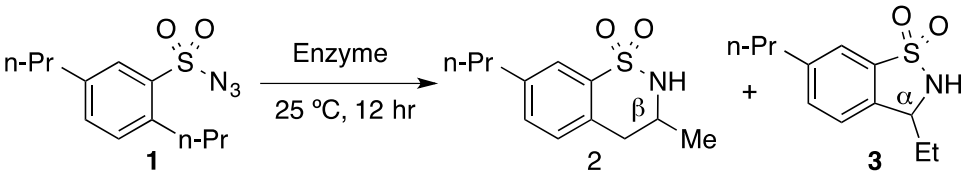

entry	Protein State	TTN[a]	**2** :**3**
1	Purified	203	91:9
2	Lyophilized whole cells	328	96:4

[a] TTN = Total turnover numbers. Enzyme = $P411_{BM3}$-CIS-T438S-I263F Reaction conditions and protein sequences described in the Supporting Information. TTNs and regioselectivities determined by HPLC analysis.

FIGURE S1. $P411_{BM3}$-CIS-T438S-I263F (blue) and $P411_{BM3}$-CIS-T438S (green) overlaid with key residues displayed and labeled.

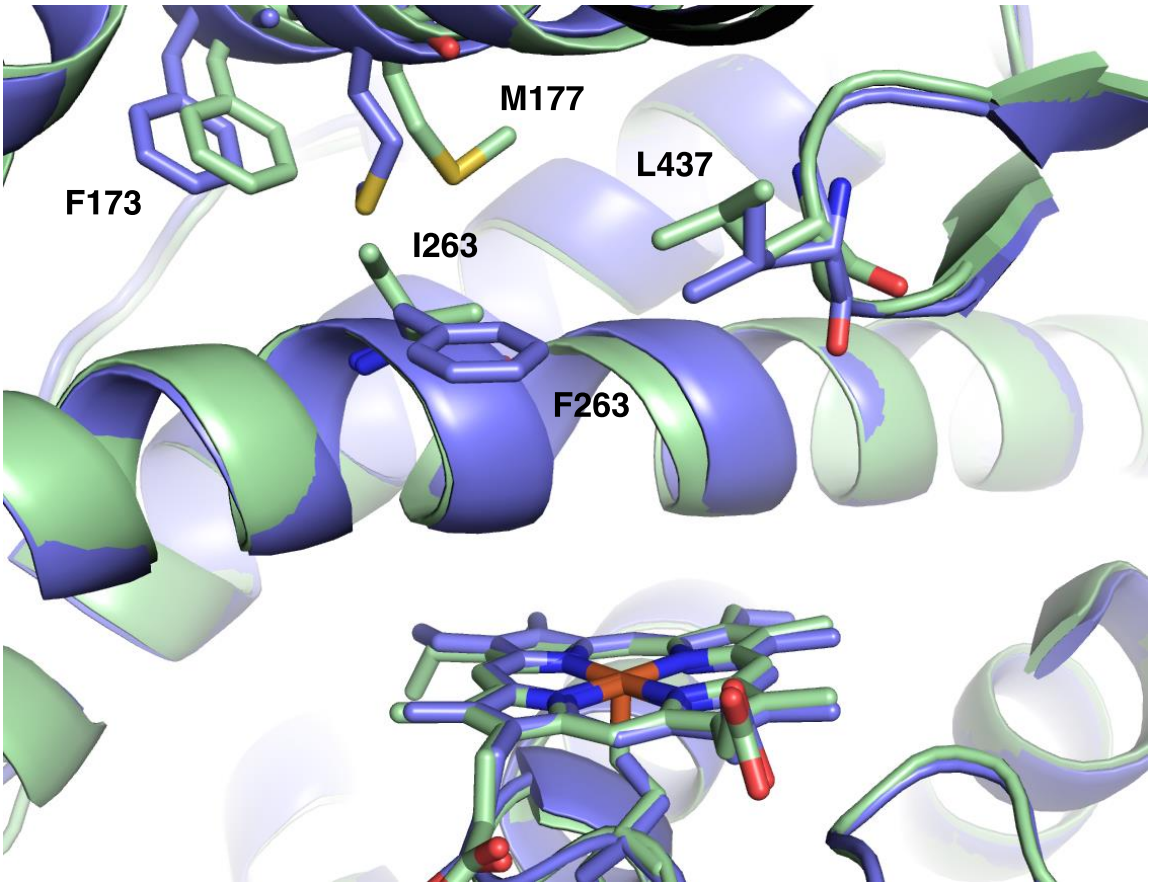

Figure S2. (Left) P411$_{BM3}$-CIS-T438S-I263F (blue) occluding C16-C18 of PAM. **(Right)** and P450$_{BM3}$ (green) containing PAM.

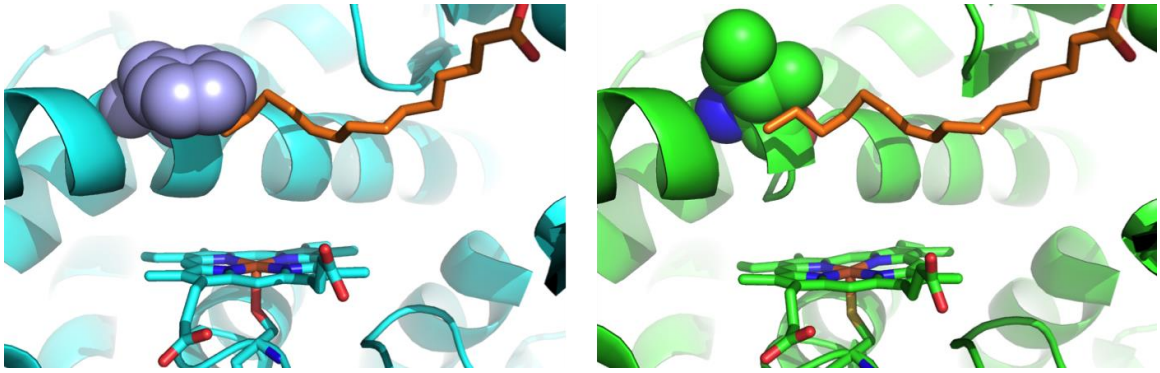

Figure S3. Initial Rate Plots of Azide **1** (blue diamonds) and Azide **1'** (red squares) with $P411_{BM3}$-CIS-T438S-I263F. Each point is an average of 3 runs

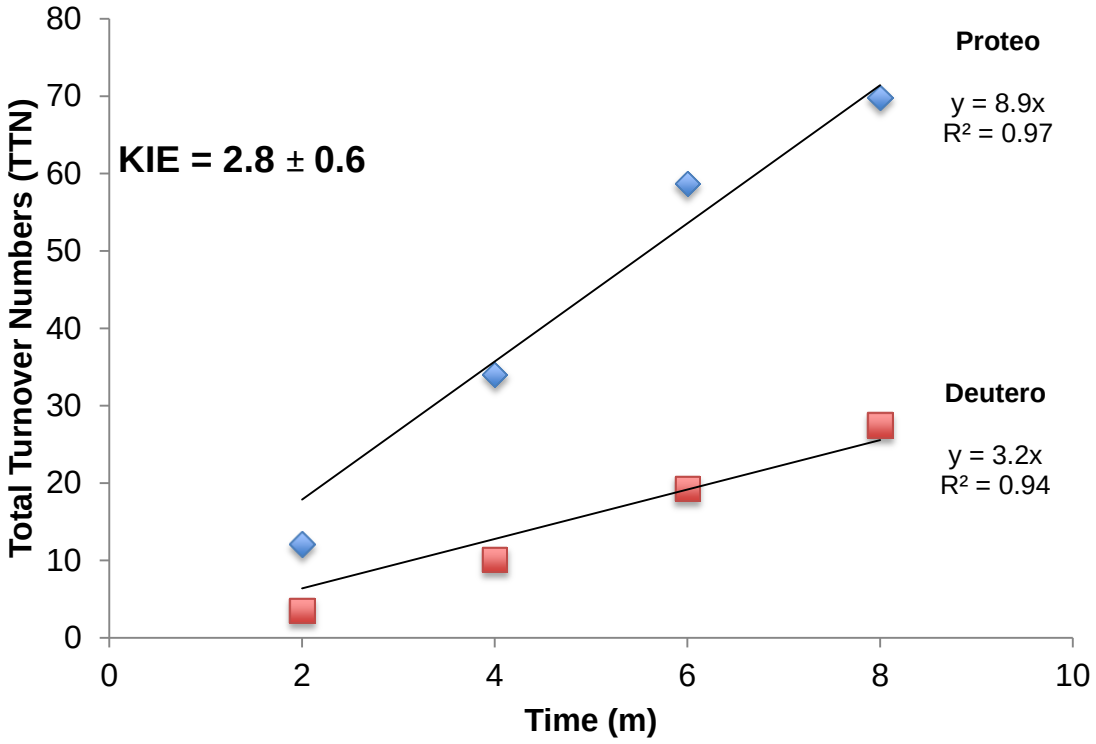

Figure S4. Initial Rate Plots of Azide **1** (blue diamonds) and Azide **1'** (red squares) with P411$_{BM3}$-T268A-F87A. Each point is an average of 3 runs

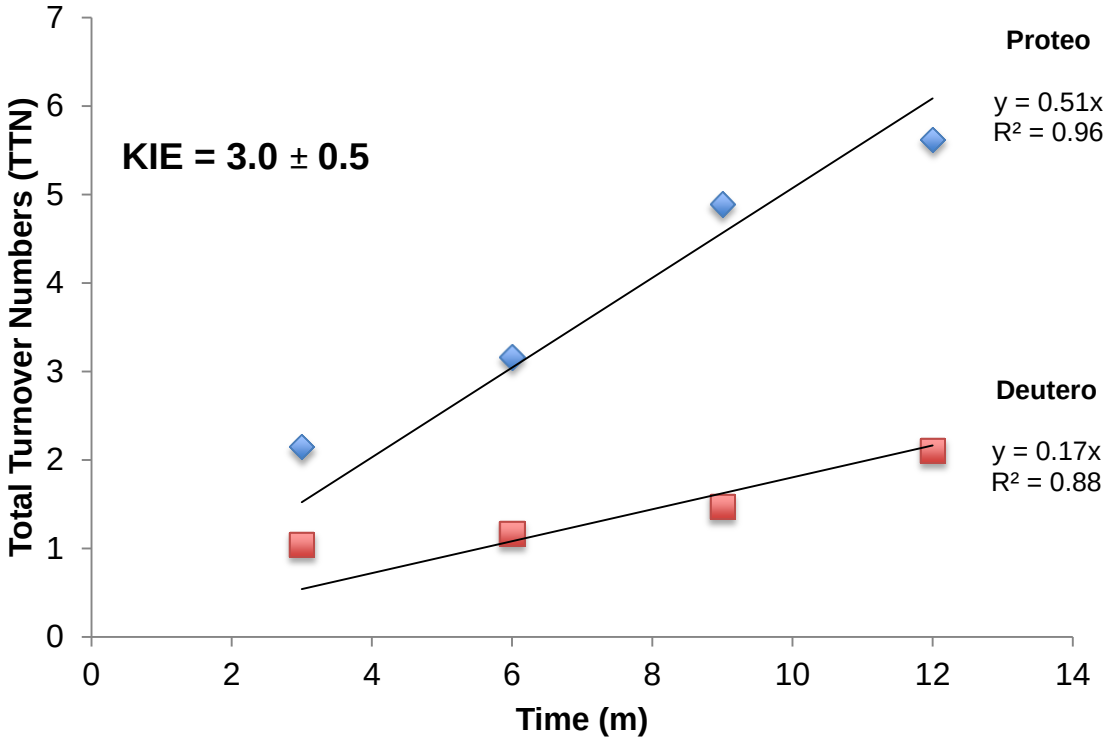

Figure S5. Docking Model of Sultam **3** covalently bound to heme with $P411_{BM3}$-CIS-T438S-I263F. Docking done using Autodock Vina.[11]

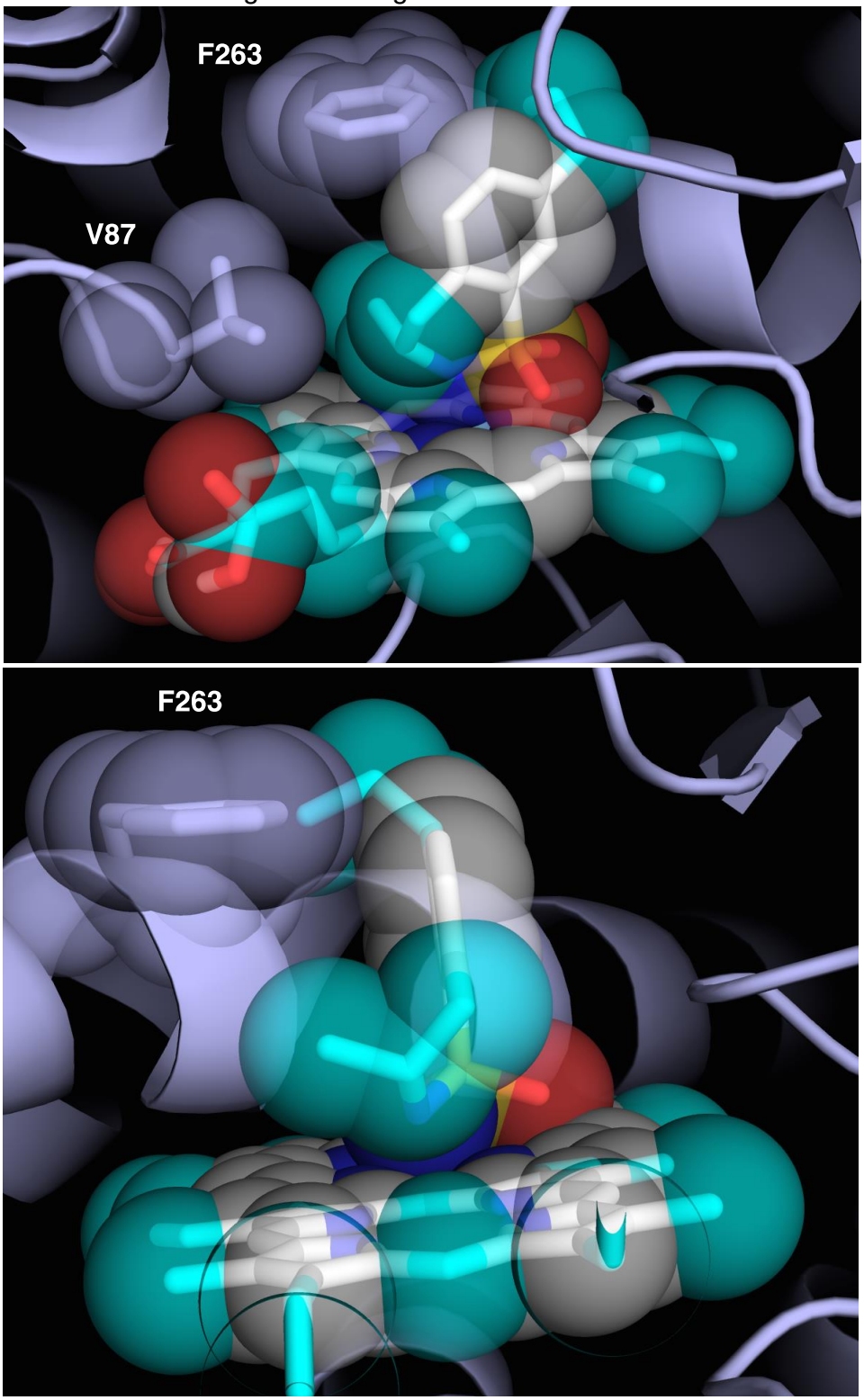

Figure S6. Regioselectivity for Conversion of Azide **1** to Sultams **2** and **3**

P411$_{BM3}$-CIS-T438S-I263F

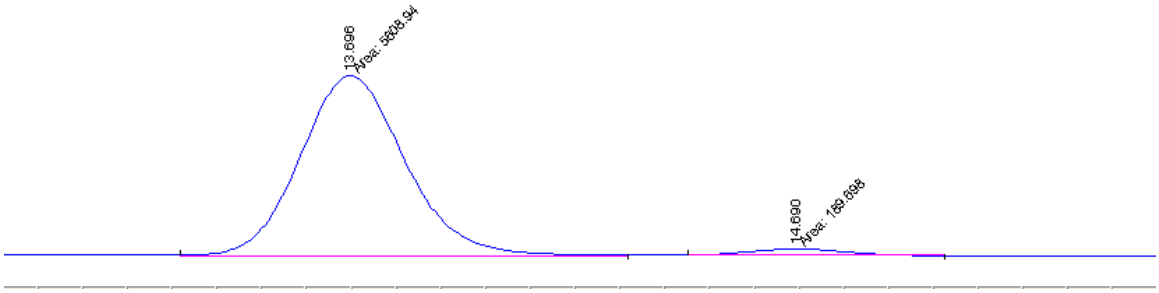

#	Time	Area	Height	Width	Area%	Symmetry
1	13.696	5608.9	341.2	0.274	96.729	0.886
2	14.69	189.7	12.3	0.258	3.271	0.959

P411$_{BM3}$-T268A-F87A

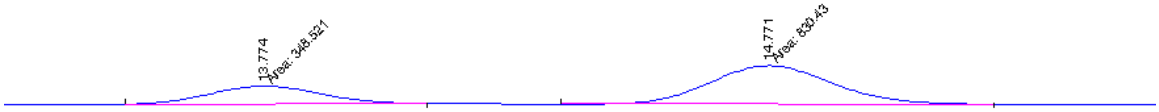

#	Time	Area	Height	Width	Area%	Symmetry
1	13.774	348.5	21.9	0.2656	29.562	1.029
2	14.771	830.4	46.7	0.2961	70.438	0.866

Figure S7. Regioselectivity for Conversion of Azide **4** to Sultams **5** and **6**

P411$_{BM3}$-CIS-T438S-I263F

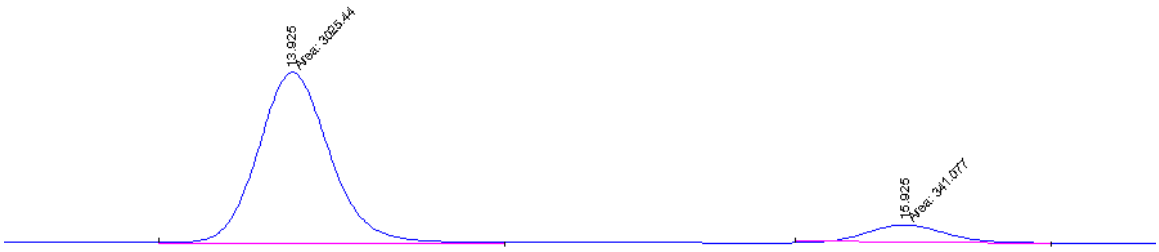

#	Time	Area	Height	Width	Area%	Symmetry
1	13.925	3025.4	184.3	0.2736	89.869	0.888
2	15.925	341.1	19	0.2994	10.131	0.848

P411$_{BM3}$-T268A-F87A

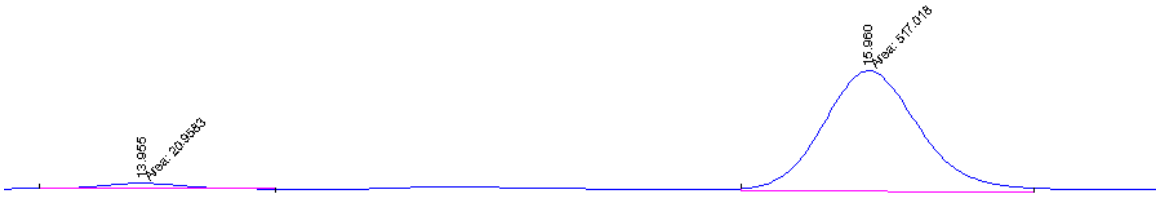

#	Time	Area	Height	Width	Area%	Symmetry
1	13.955	21	1.3	0.2715	3.896	0.901
2	15.96	517	27.5	0.3135	96.104	0.867

Figure S8. Regioselectivity for Conversion of Azide **7** to Sultams **8** and **9**

P411$_{BM3}$-CIS-T438S-I263F

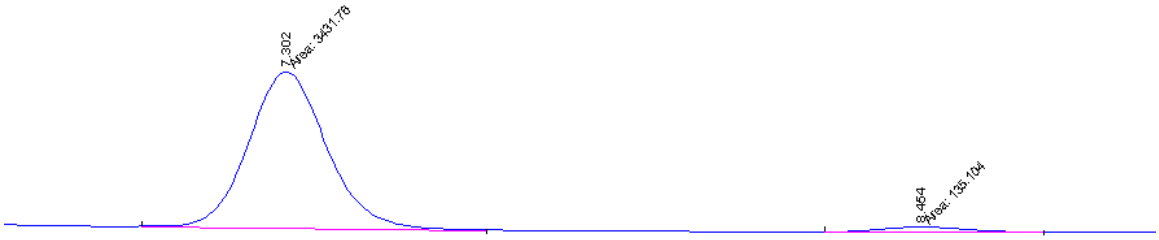

#	Time	Area	Height	Width	Area%	Symmetry
1	7.302	3431.8	345	0.1658	96.212	0.899
2	8.454	135.1	11.7	0.192	3.788	0.84

P411$_{BM3}$-T268A-F87A

#	Time	Area	Height	Width	Area%	Symmetry
1	7.395	26.7	2.8	0.1576	10.523	0.663
2	8.552	227.3	19.7	0.1924	89.477	0.825

Figure S9: Enantioselectivity Sultam **2**

Racemic

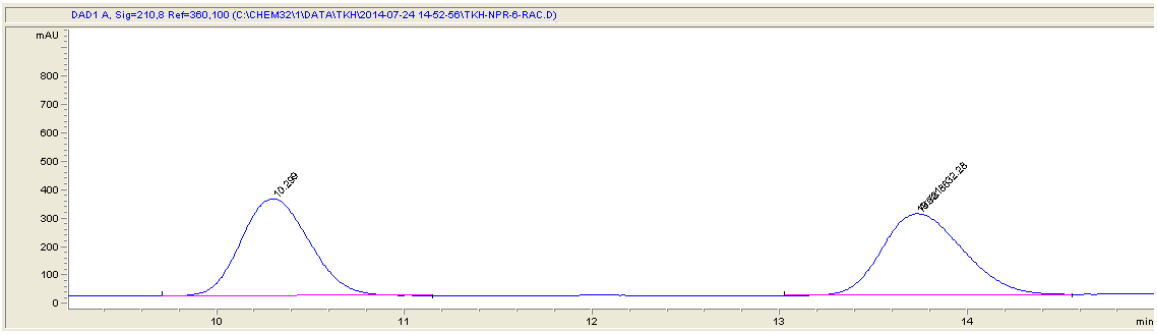

#	Time	Area	Height	Width	Area%	Symmetry
1	10.299	8654.4	340.8	0.4043	50.064	0.841
2	13.731	8632.3	287.3	0.5008	49.936	0.732

P411$_{BM3}$-CIS-T438S-I263F

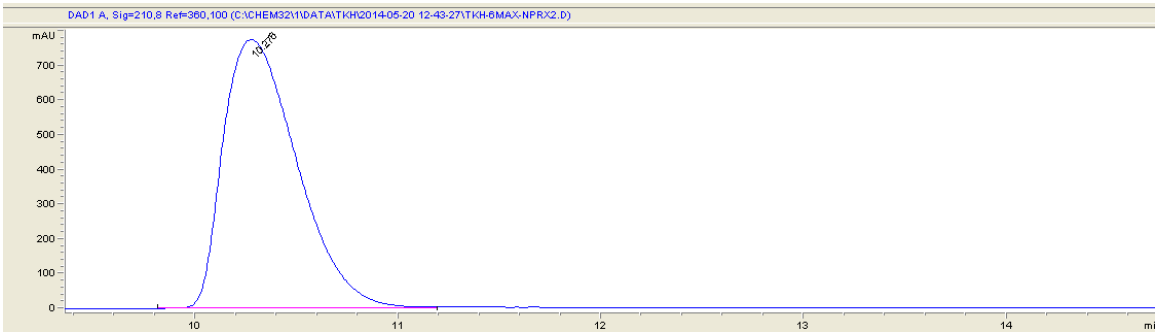

#	Time	Area	Height	Width	Area%	Symmetry
1	10.276	19619.9	774.1	0.4037	100.000	0.574

Figure S10: Enantioselectivity Sultam **3**

Racemic

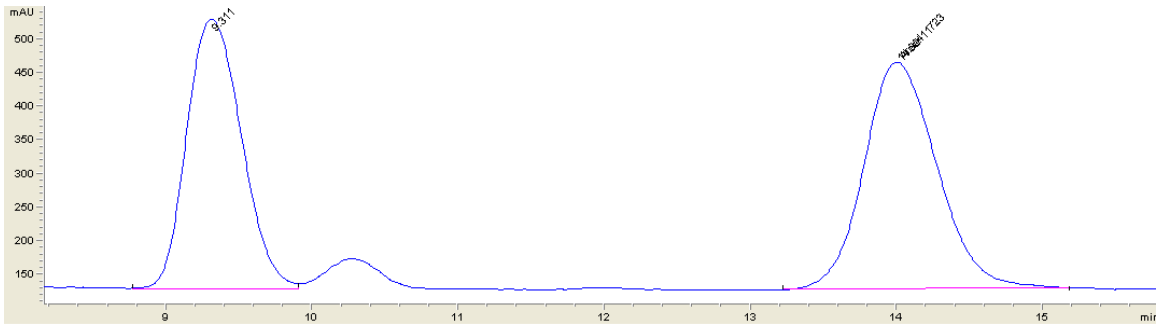

#	Time	Area	Height	Width	Area%	Symmetry
1	9.311	10519.3	401.9	0.4213	47.294	0.793
2	14.004	11723	337	0.5798	52.706	0.834

P411$_{BM3}$-T268A-F87A

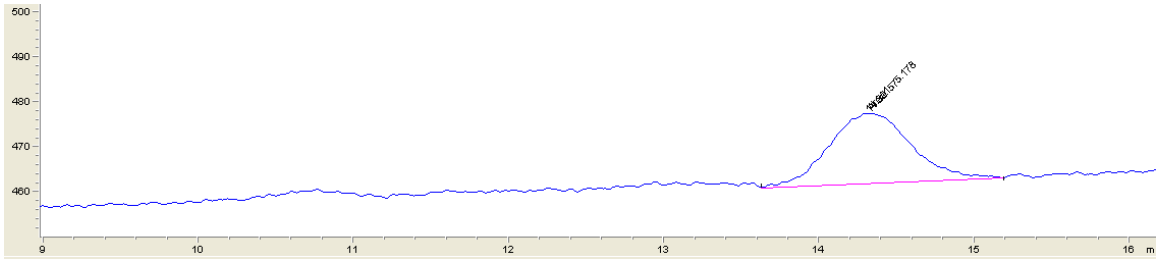

#	Time	Area	Height	Width	Area%	Symmetry
1	14.301	575.2	15.6	0.6126	100.000	0.825

Figure S11: Enantioselectivity Sultam **4**

Racemic

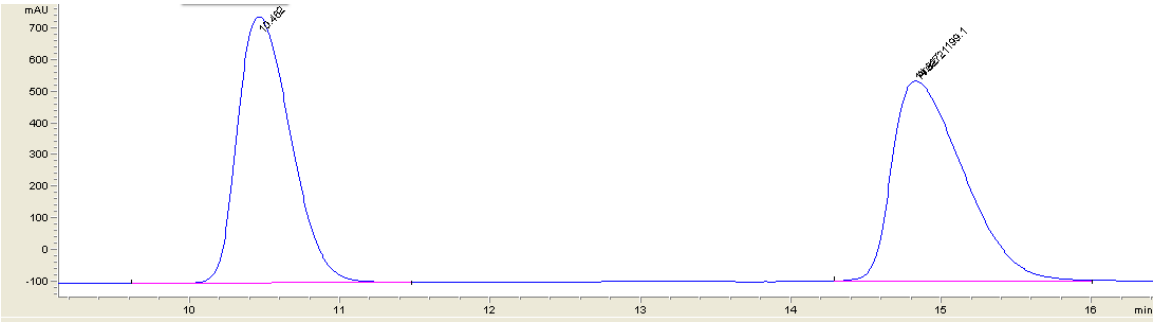

#	Time	Area	Height	Width	Area%	Symmetry
1	10.462	20623.3	841.5	0.3939	49.312	0.655
2	14.827	21199.1	636.1	0.5555	50.688	0.47

P411$_{BM3}$-CIS-T438S-I263F

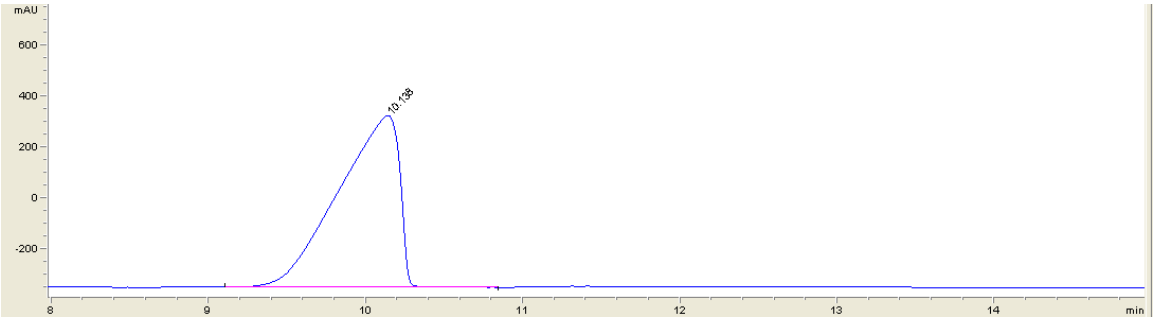

#	Time	Area	Height	Width	Area%	Symmetry
1	10.138	18376	676.1	0.4051	100.000	3.89

Figure S12: Enantioselectivity Sultam **5**

Racemic

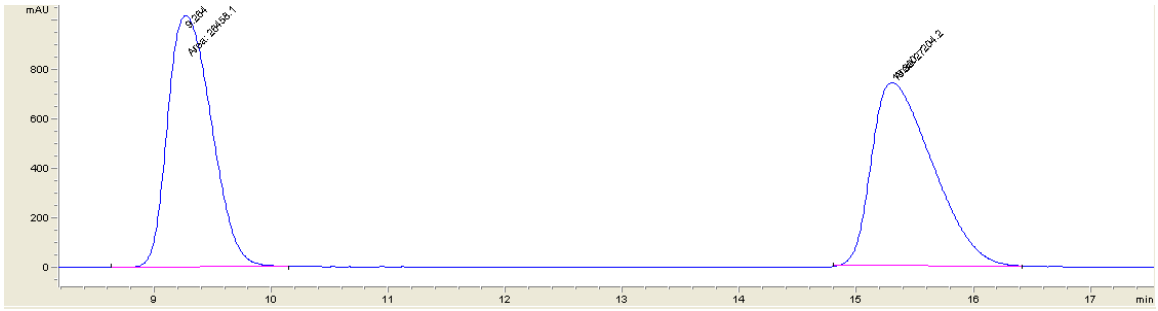

#	Time	Area	Height	Width	Area%	Symmetry
1	9.264	26458.1	1018.3	0.433	49.305	0.662
2	15.3	27204.2	744.2	0.6093	50.695	0.498

P411$_{BM3}$-T268A-F87A

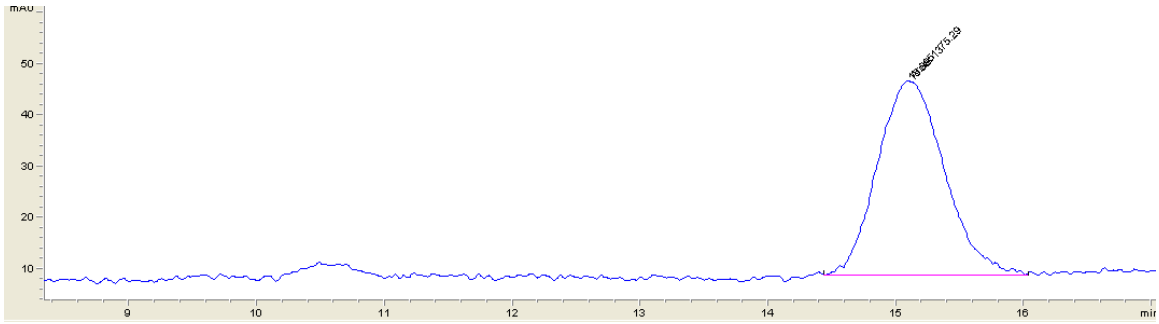

#	Time	Area	Height	Width	Area%	Symmetry
1	15.095	1375.3	37.9	0.6055	100.000	0.833

Figure S13: Enantioselectivity Sultam **8**

Racemic

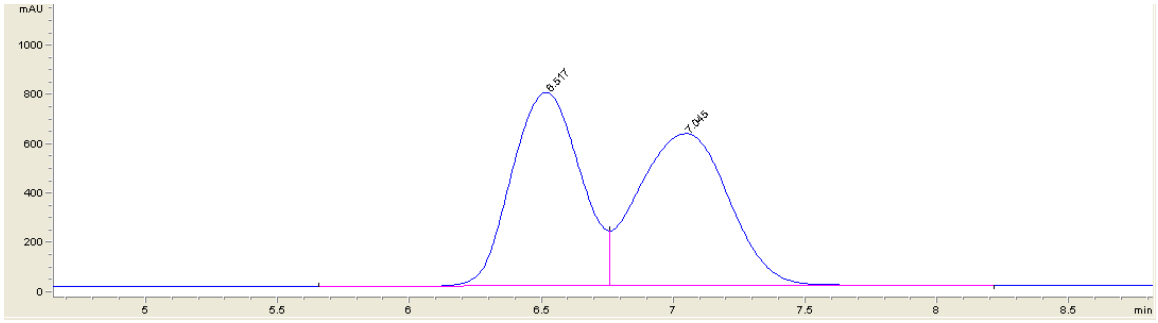

#	Time	Area	Height	Width	Area%	Symmetry
1	6.517	14273.6	787.5	0.2915	48.779	0.965
2	7.045	14988.4	618.9	0.3865	51.221	1.012

P411$_{BM3}$-CIS-T438S-I263F

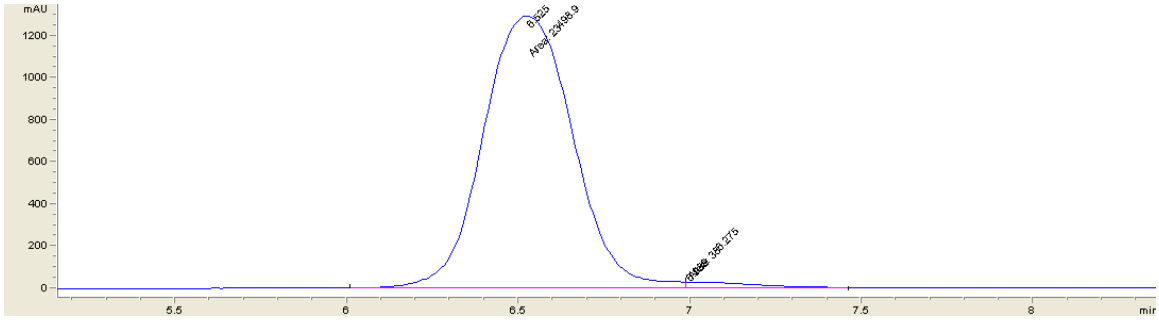

#	Time	Area	Height	Width	Area%	Symmetry
1	6.525	23498.9	1293.4	0.3028	98.383	0.925
2	6.989	386.3	28.8	0.2237	1.617	0

Figure S14: Enantioselectivity Sultam **9**

Racemic

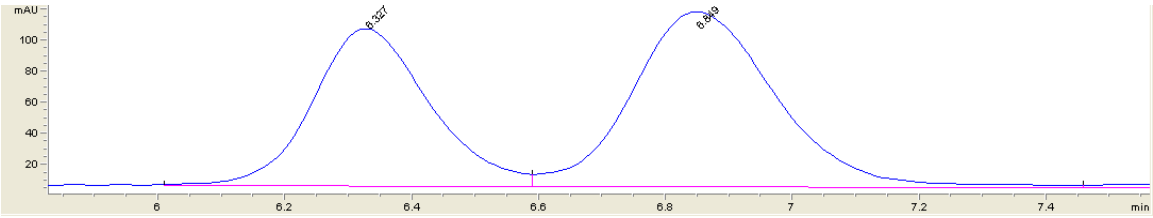

P411$_{BM3}$-T268A-F87A

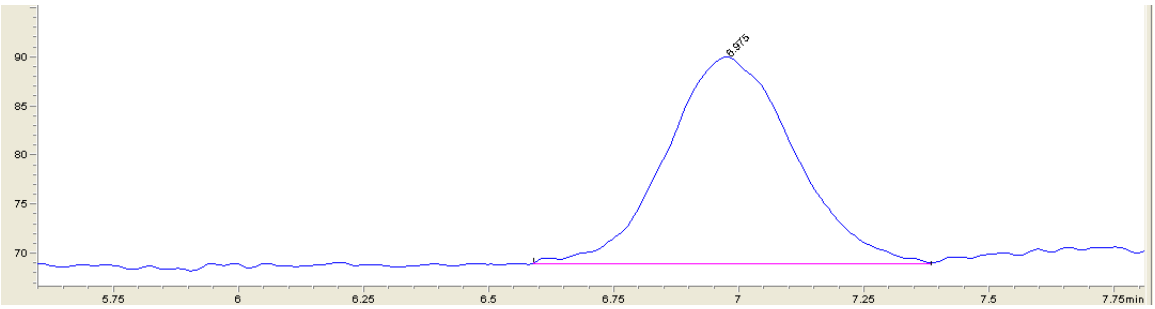

#	Time	Area	Height	Width	Area%	Symmetry
1	6.975	375.8	21.1	0.242	100.000	0.875

Figure S15: Co-Injection HPLC Traces for Sultam **2** and **3**

Synthetic

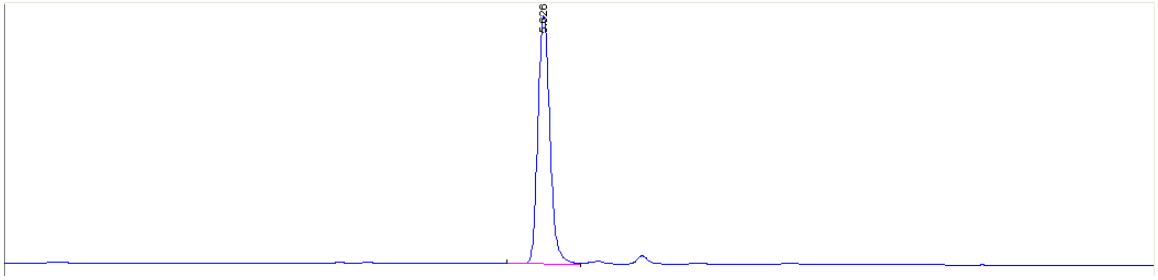

#	Time	Area	Height	Width	Area%	Symmetry
1	5.626	17394.6	1961.6	0.1395	100.000	0.863

Enzyme

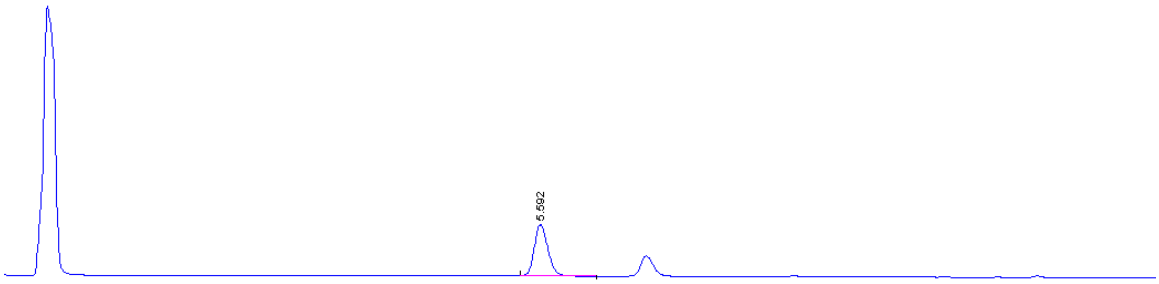

#	Time	Area	Height	Width	Area%	Symmetry
1	5.592	3930.6	394.3	0.1543	100.000	0.785

Co-injection

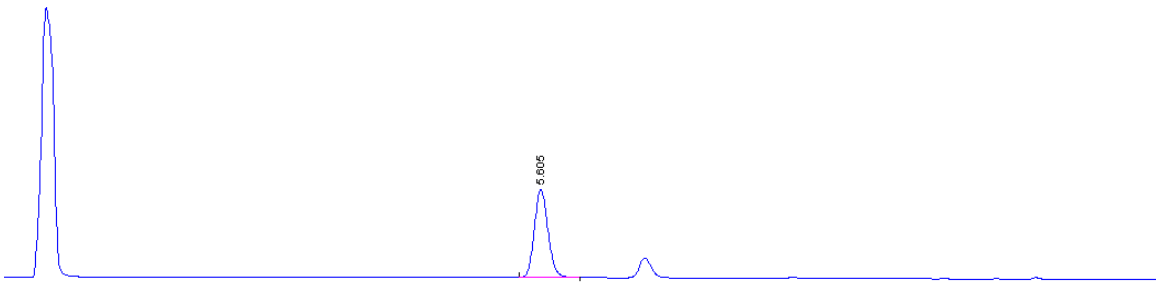

#	Time	Area	Height	Width	Area%	Symmetry
1	5.605	6833.1	682.9	0.1547	100.000	0.849

Figure S16: Co-Injection HPLC Traces for Sultam **5** and **6**

Synthetic

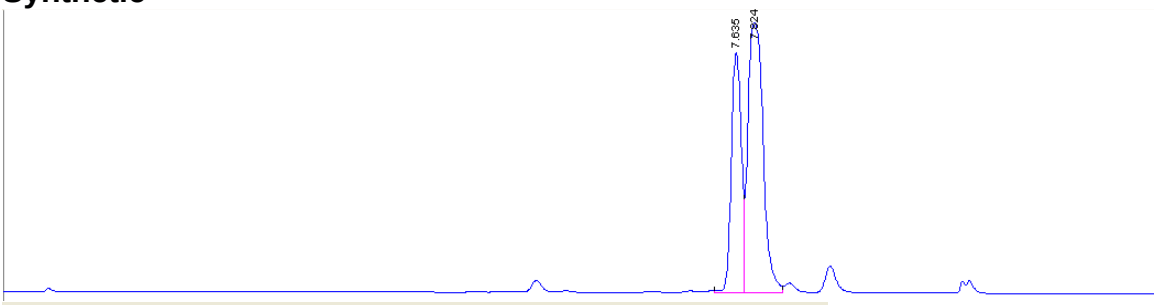

#	Time	Area	Height	Width	Area%	Symmetry
1	7.635	16087.5	2197.7	0.1154	37.108	0.964
2	7.824	27265.7	2466	0.175	62.892	0.678

Enzyme

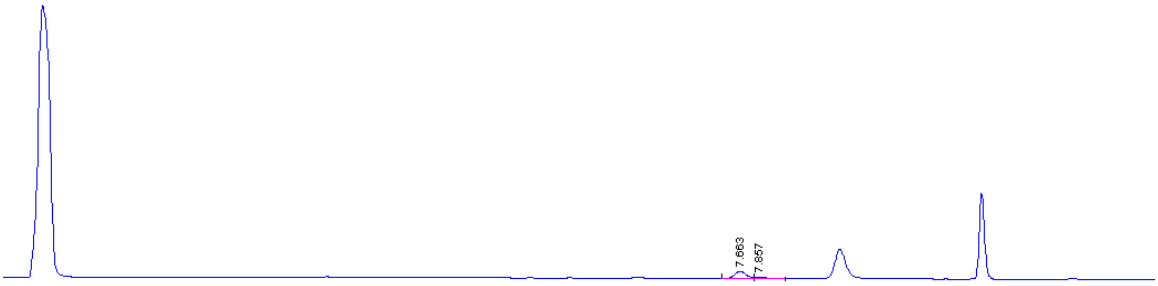

#	Time	Area	Height	Width	Area%	Symmetry
1	7.663	468.9	55.7	0.1282	79.806	0.828
2	7.857	118.7	11	0.1524	20.194	0.287

Co-injection

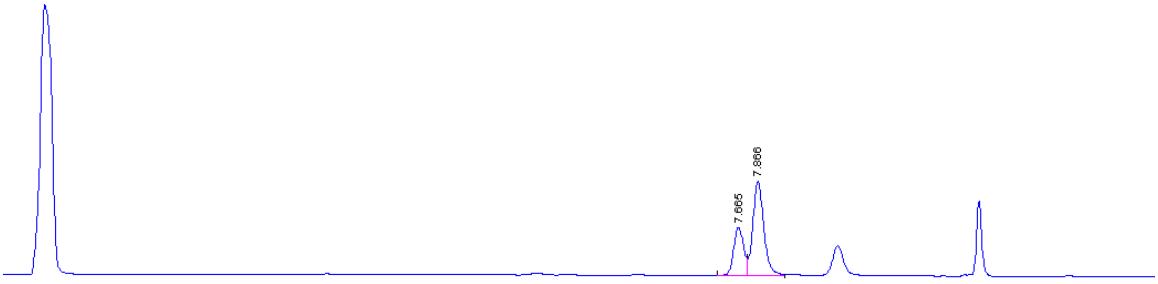

#	Time	Area	Height	Width	Area%	Symmetry
1	7.665	2679.1	367.6	0.111	31.648	0.947
2	7.866	5786.1	720.4	0.1217	68.352	0.795

Figure S17: Co-Injection HPLC Traces for Sultam **8** and **9**

Synthetic

#	Time	Area	Height	Width	Area%	Symmetry
1	3.863	1614.4	237.6	0.1132	69.342	0.944
2	4.009	713.8	95.3	0.1248	30.658	0.694

Enzyme

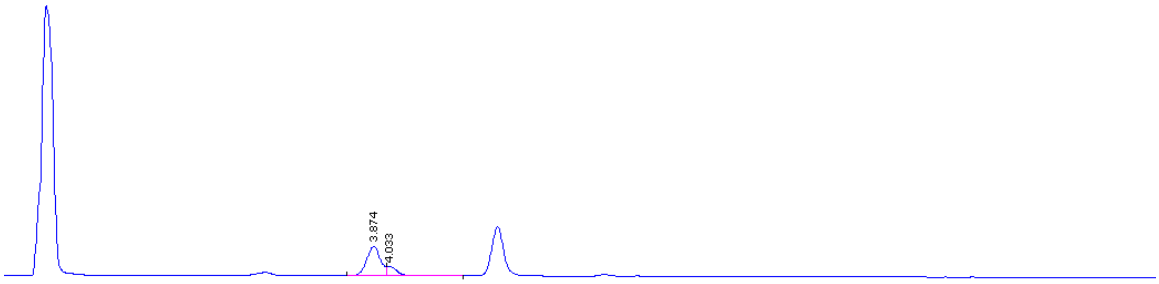

#	Time	Area	Height	Width	Area%	Symmetry
1	3.874	2329.6	230.1	0.1521	83.139	0.993
2	4.033	472.5	70.7	0.1114	16.861	0.171

Co-injection

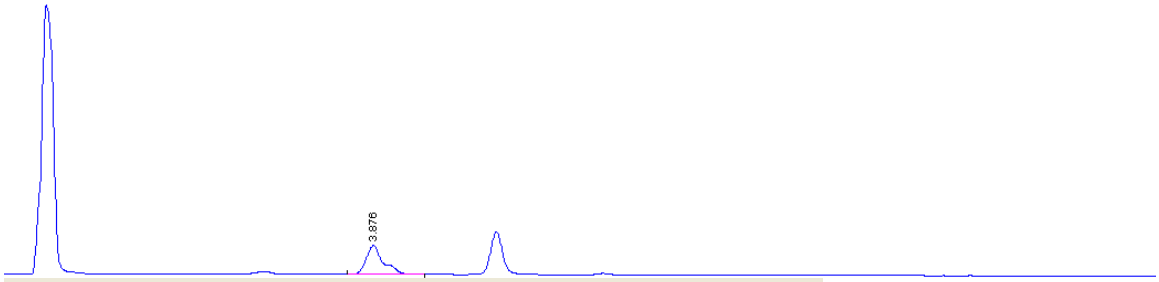

#	Time	Area	Height	Width	Area%	Symmetry
1	3.876	2902	235.9	0.1775	100.000	0.67

Figure S18: LC-MS Traces for Sultams **2** + **3**

Predicted M+H = 240.1
Observed M+H = 240.1

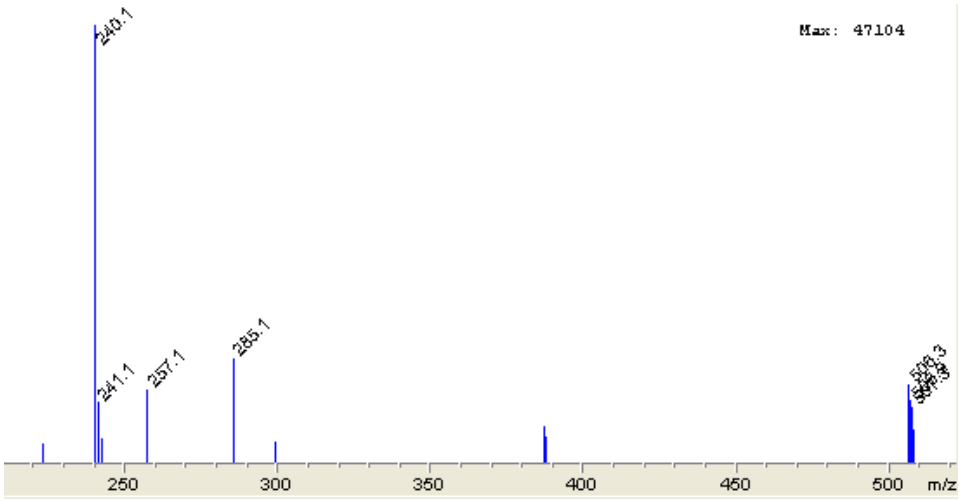

Figure S19: LC-MS Traces for Sultams **5** + **6**

Predicted M+H = 268.1
Observed M+H = 268.1

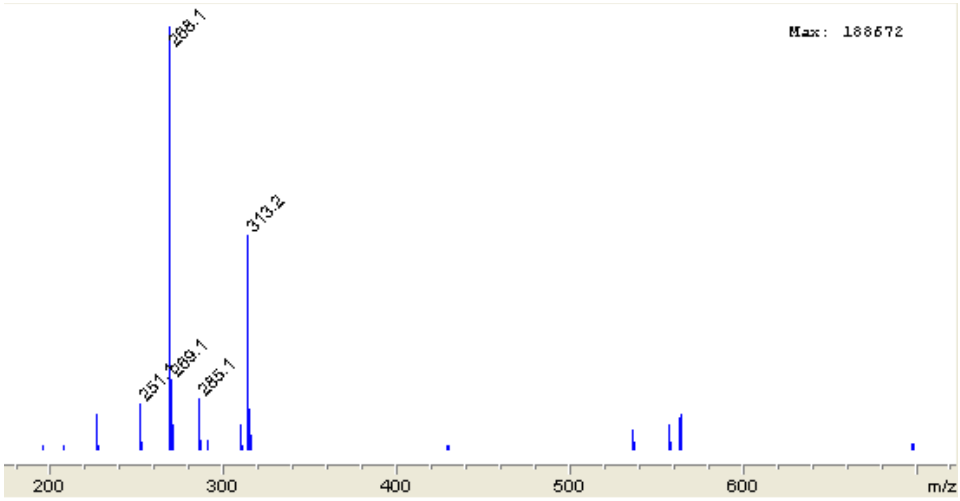

Figure S20: LC-MS Traces for Sultams **8** + **9**

Predicted M+H = 270.1
Observed M+H = 270.1

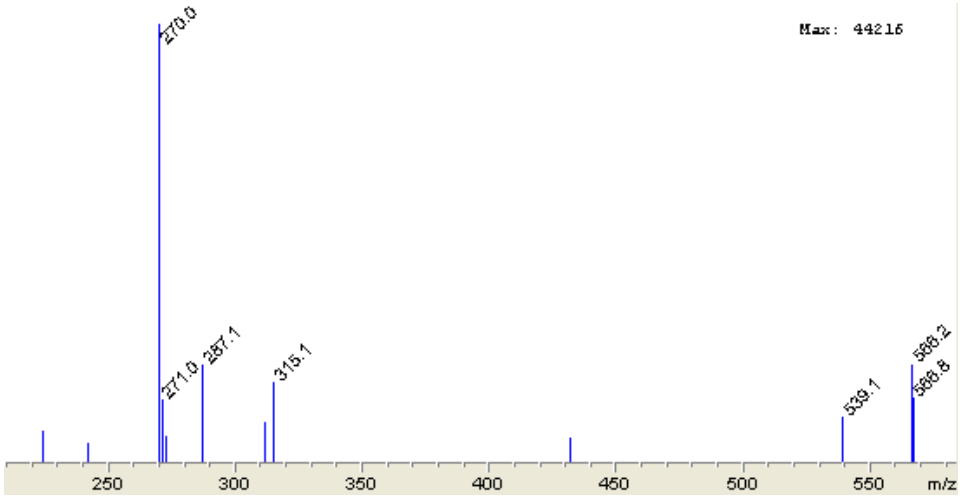

Figure S21: Calibration Curves for Sultam Products

Sultam **2** and **3**

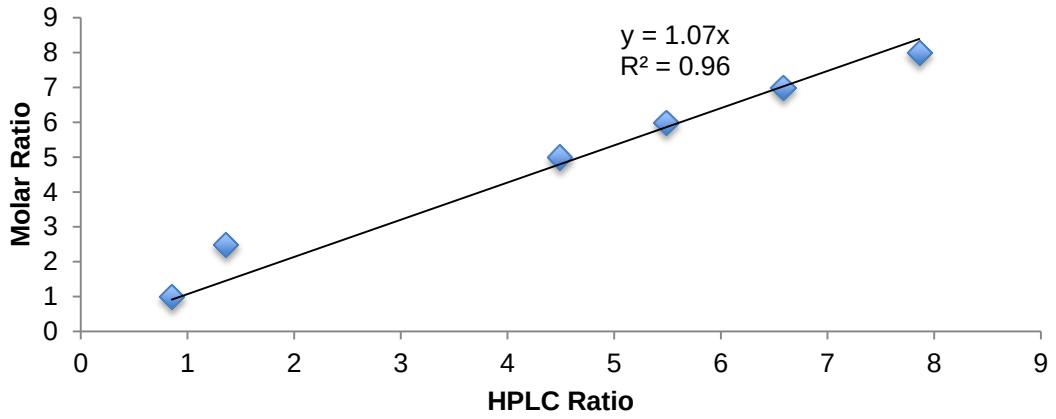

Sultam **5** and **6**

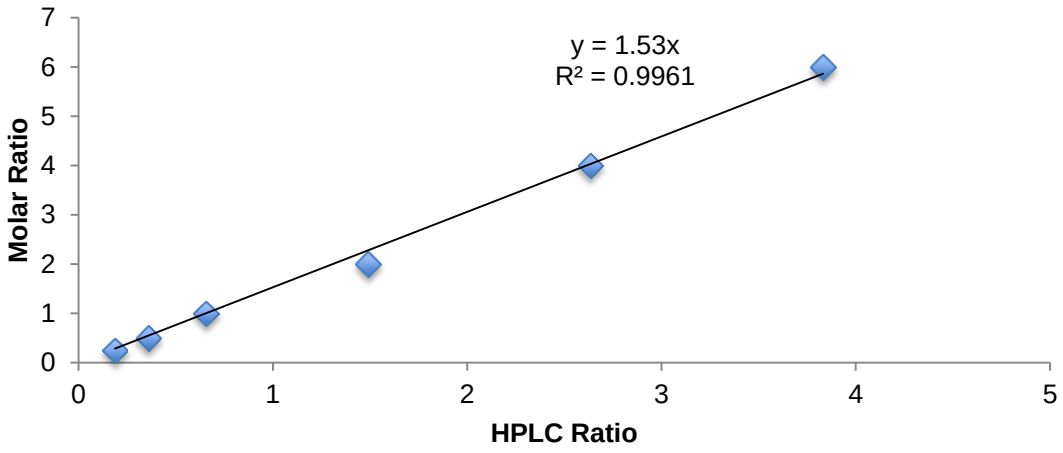

Sultam **8** and **9**

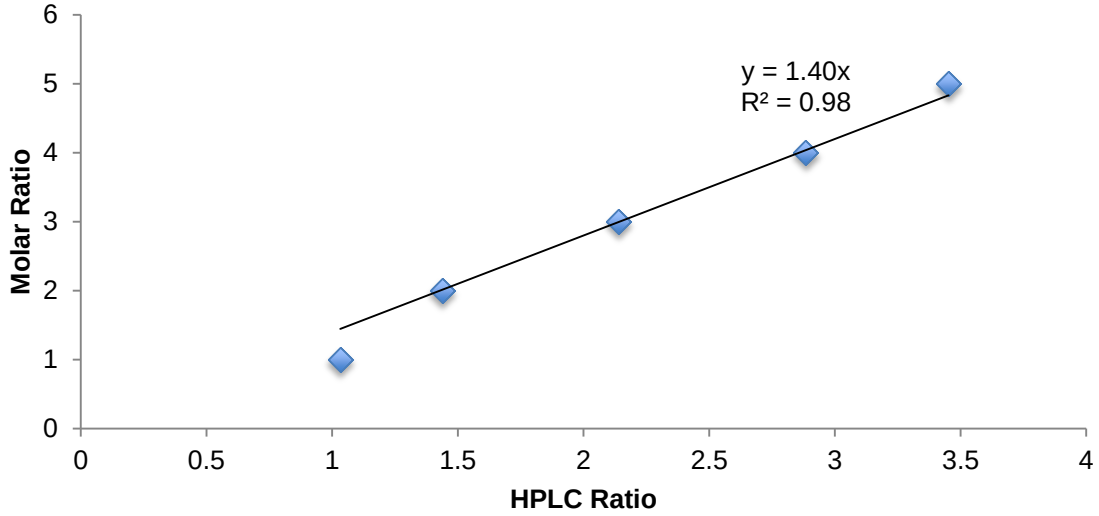

[1] Ruppel, J. C.; Kamble, R. M.; Zhang, X. P. *Org. Lett.* **2007**, *9*, 4889-4892.
[2] Coelho, P. S.; Brustad, E. M.; Kannan, A.; Arnold, F. H. *Science* **2013**, *339*, 307.
[3] S. Kille, C. G. Acevedo-Rocha, L. P. Parra, Z.-G Zhang, D. J. Opperman, M. T. Reetz, J. P. Acevedo, *ACS Synth. Biol.* **2013**, *2*, 83–92.
[4] Kabsch, W. *Acta Cryst.* **2010**, D*66*, 125.
[5] McCoy, A. J.; Grosse-Kunstleve, R. W.; Adams, P. D.; Winn, M. D.; Storoni, L. C.; Read, R. J. *J. Appl. Cryst.* **2007**, *40*, 658.
[6] Bailey, S. *Acta Cryst.* **1994**, D*50*, 760.
[7] (a) Emsley, P.; Cowtan, K. *Acta Cryst.* **2004**, D*60*, 2126. (b) Winn, M. D.; Murshudov, G. N.; Papiz, M. Z. *Macromolecular Crystallography, Pt D* **2003**, *374*, 300.
[8] Chen, V. B. ; Arendall III, W. B.; Headd, J. J.; Keedy, D. A.; Immormino, R. M.; Kapral, G. J.; Murray, L. W.; Richardson, J. S.; Richardson, D. C. *Acta Cryst.* **2010**, D*66*, 12.
[9] Painter, J.; Merritt, E. A. *J. Appl. Cryst.* **2006**, *39*, 109.
[10] Ichinose, M.; Suematsu, H.; Yasutomi, Y.; Nishioka, Y.; Uchida, T.; Katsuki, T. *Angew. Chem. Int. Ed.* **2011**, *50*, 9884-9887.
[11] Trott, O.; Olson, J. A. *J. Comp. Chem.* **2010**, *31*, 455.